EVS30 Symposium
Stuttgart, Germany, October 9 - 11, 2017

Model-Based Optimization of a Plug-In Hybrid Electric Powertrain with Multimode Transmission

Stefan Geng, Andreas Meier and Thomas Schulte

Ostwestfalen-Lippe University of Applied Sciences

Liebigstraße 87, 32657 Lemgo, Germany

E-Mail: {stefan.geng, thomas.schulte}@hs-owl.de

Summary

Plug-in hybrid electric vehicles are developed to reduce the fuel consumption and the emission of carbon dioxide. Besides the series, parallel and power split configurations as commonly used for conventional hybrid electric vehicles, multimode transmissions are used for plug-in hybrid electric vehicles, which enable to switch between different modes like parallel or series operation of combustion engine and electric motor. Several concepts have already been discussed and presented. These concepts comprise novel structures and multi-speed operation for the combustion engine and the electric motor, respectively.

For improving the fuel and energy consumption, model-based optimizations of multimode transmissions are performed. In the first step of the optimization, the optimal number of gears and transmission ratios as well as the corresponding fuel and energy savings are estimated. Based on these results a new multimode transmission concept with two-speed transmissions for the combustion engine and the electric motor was developed. The knowledge of the concrete concept enables further optimizations of the transmission ratios and the transmission control. In order to prove the benefit of the new and optimized transmission concept, powertrain simulations are carried out. The new powertrain concept is compared to a powertrain concept with single-speed transmissions for the ICE and electric motor operation. The new transmission concept enables a significant improvement of the fuel consumption.

Keywords: PHEV (plug-in hybrid electric vehicles), Transmission, Optimization, Simulation, Efficiency

1 Introduction

Today, vehicle manufacturers are forced to reduce the fuel consumption of their products due to enhanced environmental regulations. A promising solution is the development of plug-in hybrid electric vehicles (PHEV) since they combine an extended electric cruising range and the possibility to propel the vehicle by an internal combustion engine (ICE) when the battery is depleted or high performance is required (e. g. on highways). Common powertrain configurations of PHEVs are the series-, parallel- and power split configurations. The efficiencies of these configurations vary depending on the distance and the power demand of the trip that will be made [1]. For this reason, special transmission concepts are developed, which enable to switch the operation mode of the powertrain. Each operation mode conforms one of the common powertrain configurations and the capability of switching them during the vehicle operation will combine the advantages of the available powertrain configurations.

These so called multimode or dedicated hybrid transmissions (DHT) are optimized for the application in PHEVs. Compared to add-on solutions, where the electric motor is added to a conventional automatic transmission, DHTs are less complex (less speeds) and the electric motors are an integral part of the transmission. A simple and compact transmission design saves space and weight, which in turn compensates a part of the additional space and weight of the electric motors and the battery. It also reduces the costs of the overall powertrain and makes PHEVs increasingly economic for customers. A general property of DHTs is that the electric motor is indispensable for the operation of the overall powertrain [2]. Some vehicle manufacturers already offer DHTs, e.g. the Toyota with the 4th generation of the Prius [3], GM with the “Voltec” system [4] or Mitsubishi with the multimode transmission [5]. Figure 1 shows the concept of the multimode transmission, where the electric motor and the ICE are connected to the final drive by means of fixed transmission ratios. Depending on the state of the clutch, the transmission enables a series hybrid mode, a parallel hybrid mode, an electric driving mode and an ICE mode. Due to the fixed gear ratio, the ICE can be operated with a mechanical coupling to the final drive, only at relatively high vehicle speeds. At lower speeds, the vehicle can be driven by the electric motor, only and the series hybrid mode is necessary when the battery is depleted. Consequently, without the electric motor, the whole powertrain concept would be inoperatively.

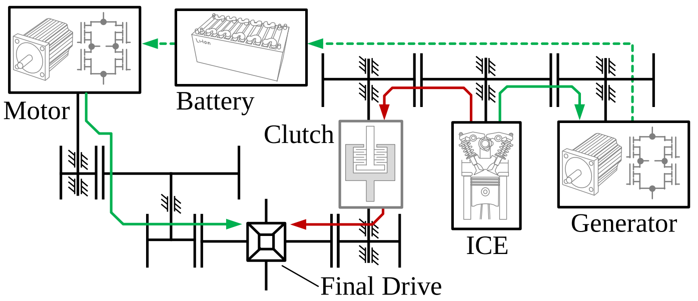

Mode	Clutch State
series	disengaged
electric driving	disengaged
parallel	engaged
ICE	engaged

Figure 1: Multimode transmission with fixed gear ratios for the ICE and electric motor.

In this contribution, a model-based development of a new DHT concept is presented. As general basis for the development, a vehicle similar to the Mitsubishi Outlander is considered. Unlike the powertrain concept of the Mitsubishi Outlander (see, Figure 1), the new concept will comprise only one electric motor. In order to exploit the maximum efficiency of the transmission concept, a model-based optimization of the number of speeds and the related transmission ratios is carried out. The properties of all powertrain components (ICE, electric motor, battery and vehicle dynamics) are chosen similar to the Mitsubishi Outlander and they are no subject to the optimization.

The powertrain model as well as the considered powertrain components and its parametrization are presented in chapter 2. Chapter 3 contains the optimization of the number of speeds and a first estimation of the transmission ratios. Based on these results a new transmission concept was developed which is presented in chapter 4. Due to the knowledge of the specific transmission configuration, a further optimization of the transmission ratios is carried out. The second optimization step requires an operation strategy, which defines the optimal control trajectory of the powertrain. A description of the method used to determine the optimal control trajectory is also contained in chapter 5. Finally, the new transmission concept is evaluated by comparing simulation results of the optimized concept with those of the concept shown in Figure 1.

2 Powertrain Model

An appropriate modelling approach for the purpose of optimization needs to combine a good adaptability of system parameters as well as low computational effort. This is obtained by the so-called backward approach [6], where beginning with the requested acceleration a_{veh} and speed v_{veh} of the vehicle, the operating states of each powertrain component are determined backwards, see Figure 2. It is always assumed that the ICE and the electric motors are capable to generate the required torque and satisfying the requested vehicle acceleration, respectively. The submodels of the powertrain components consider the stationary states only, which is why no controllers for the powertrain components are required. Nevertheless, since a PHEV is considered, the operation mode for the powertrain must be controlled. The operation mode s_{m} is set by the operating strategy, which controls the transmission and also the ICE or electric motor. E.g. in parallel hybrid mode, the torque-split between the ICE and electric motor needs to be controlled (output $\tilde{\mathbf{u}}$ in Figure 2). Since no dynamic behavior is considered, the operation mode changes immediately without any transition (e.g. continuously changing the state of a clutch from engaged to disengaged). The output of the powertrain simulation is the mass flow rate of fuel $\dot{m}_{\mathrm{f}}$ and the state of charge of the battery SoC.

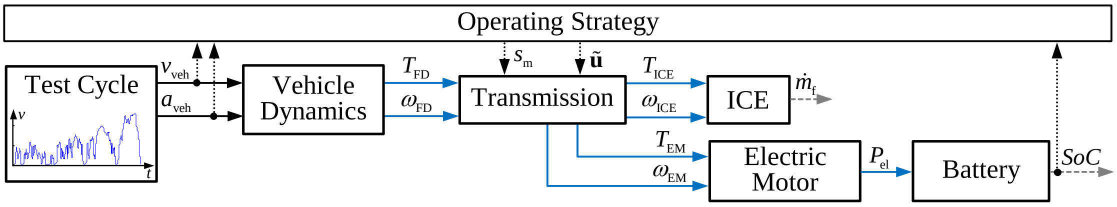

Figure 2: Powertrain model according to the backward approach.

Figure 3 shows the submodels of the powertrain and their most significant parameters. The vehicle dynamics, is considered in longitudinal direction only, where the torque at the final drive is determined according to

$$T_{\mathrm{FD}} = r_{\mathrm{w}} \cdot \left(F_{\mathrm{drag}} \left(v_{\mathrm{veh}} \right) + F_{\mathrm{roll}} + F_{\mathrm{downhill}} + m_{\mathrm{veh}} \cdot a_{\mathrm{veh}} \right) \tag{1}$$

with the radius of the wheels r_{w}, the vehicle speed v_{veh} and the vehicle acceleration a_{veh} (extracted from the test cycle). The forces in (1) represent the driving resistances comprising the drag force F_{drag}, the rolling friction force F_{roll} and the downhill force F_{downhill}. By means of the torque T_{FD} and the rotational speed ω_{FD} at the final drive, the transmission model can be evaluated. It determines the torques and rotational speeds of the ICE and the electric motor by considering the operation mode and the transmission ratios. An automatic model generation is used to generate a transmission model according to

$$\left[T_{\mathrm{ICE}} \ T_{EM} \ \omega_{\mathrm{ICE}} \ \omega_{EM} \right]^T = \mathbf{f}_{\mathrm{Trans}} \left(T_{\mathrm{FD}}, \omega_{\mathrm{FD}}, s_m, \tilde{u} \right) \tag{2}$$

where the degree of detail (e.g. transmission dynamics, drag and friction losses, …) is adjustable [7]. In this contribution (2) is a stationary function with the operation mode s_{m} and the input $\tilde{u}$ containing the desired torque or rotational speed for the electric motor (only when necessary: e.g. torque-split in parallel hybrid mode).

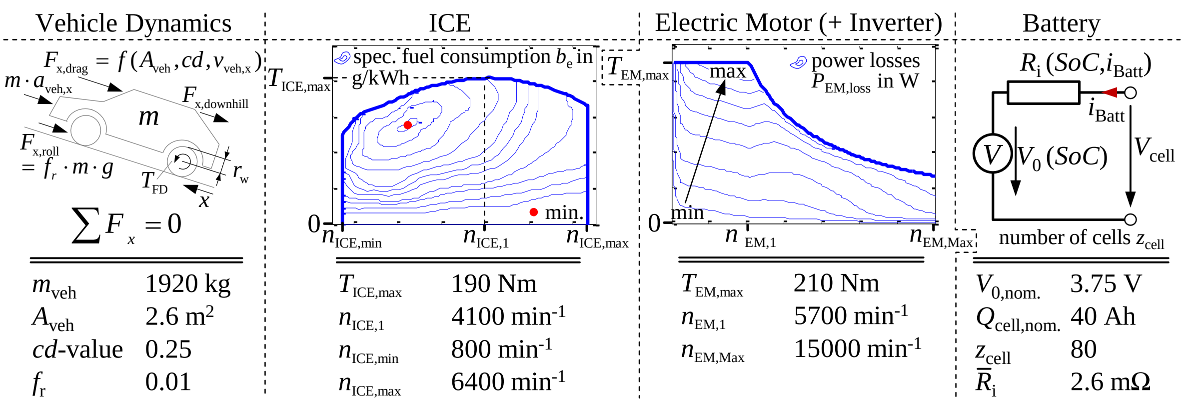

Figure 3: Submodels of the powertrain components and the most significant parameters.

The ICE is represented by a map, which describes the specific fuel consumption b_e as a function of torque and rotational speed. The mass flow rate of the fuel is determined according to

$$\dot{m}_\mathrm{f} = \frac{b_\mathrm{e}\left(T_\mathrm{ICE}, \omega_\mathrm{ICE}\right) \cdot T_\mathrm{ICE} \cdot \omega_\mathrm{ICE}}{3.6 \cdot 10^6} \tag{3}$$

with $\dot{m}_\mathrm{f}$ in $g \cdot s^{-1}$. Similarly, the required electric power P_el of the electric motor is determined:

$$P_\mathrm{el} = T_\mathrm{EM} \cdot \omega_\mathrm{EM} + P_\mathrm{EM,loss}\left(\left|T_\mathrm{EM}\right|, \left|\omega_\mathrm{EM}\right|\right) \tag{4}$$

where the power loss $P_\mathrm{EM,loss}$ is a result of the map shown in Figure 3. This map also includes the power losses of the inverter. Since the electric power P_el must be provided by the battery, a battery current

$$\dot{q} = i_\mathrm{Batt} = -\frac{V_0\left(SoC\right)}{R_\mathrm{i}\left(SoC\right)} + \sqrt{\left(\frac{V_0\left(SoC\right)}{R_\mathrm{i}\left(SoC\right)}\right)^2 - \frac{P_\mathrm{el}}{z_\mathrm{cell}}} \tag{5}$$

will occur. Equation (5) follows from the simplified equivalent circuit in Figure 3, where z_cell is the number of cells, V_0 the internal cell voltage and R_i the internal cell resistance. In this representation V_0 and R_i are a function of the state of charge

$$SoC = \frac{100}{3600} \cdot \int \frac{i_\mathrm{Batt}}{z_\mathrm{cell} \cdot Q_\mathrm{cell,nom}}\, dt \tag{6}$$

only, which is determined by integrating (5) and dividing the result by the nominal battery capacity. Since the powertrain model is executed in discrete time steps, (5) can be solved explicitly (no algebraic loop occur).

For the optimization in the following chapter, the powertrain model described above is used and parameterized according to Figure 3. The second optimization step in chapter 5 requires a convex powertrain model, which is approximates the model above. Because the transmission concept is refined in each optimization step, several transmission models with different degree of detail are used. A short description of the used transmission model is given in the corresponding chapters.

3 Optimization: Number of Speeds

In this chapter, the impact of the number of speeds for the ICE and electric motor operation on the fuel and energy consumption is investigated. Since no specific transmission concept is known within this stage of development, a simplified transmission model is used. It represents two separate transmission ratios: one for the ICE and one for the electric motor. Both transmission ratios can be switched during simulation in order to represent multi-speed transmissions.

For this investigation the operation of the ICE and the electric motor is considered separately, i.e. the energy for propelling the vehicle comes from either the fuel or the battery. It is intended to analyze the benefit of multiple speeds for each power source and to estimate the optimal number of speeds. Furthermore, it is assumed that the impact of multiple speeds for the combined operation of the ICE and electric motor is comparable to that of the separated consideration. If only one power source is considered, the optimal shift strategy (choice of the optimal gear s_g) can be determined without considering any specific test cycle. Therefore, the optimal choice of the gear s_g is determined according to

$$P_\mathrm{loss}\left(v_\mathrm{veh}, T_\mathrm{FD}, s_\mathrm{g}^*\right) = \min_{s_\mathrm{g} \in \mathbb{N}} P_\mathrm{loss}\left(v_\mathrm{veh}, T_\mathrm{FD}, s_\mathrm{g}\right). \tag{7}$$

where the overall power loss within the powertrain P_loss is minimized for all possible final drive torques T_FD and vehicle speeds v_veh. As a result, a map which defines the optimal choice of the gear $s_\mathrm{g}^*\left(T_\mathrm{FD}, v_\mathrm{veh}\right)$ is obtained. Since the number of possible solutions for (7) is equal to the number of speeds, a feasible and still fast method for solving (7) is to check all possibilities and choose the best one.

Figure 4a shows the procedure for optimizing the transmission ratios of a multi-speed transmission in terms of a minimal fuel and energy consumption, respectively. The simplex method is applied to find the optimal set of transmission ratios $\mathbf{i}_{\mathrm{ICE,EM}}$, which causes the lowest consumption for a given test cycle. For each set of $\mathbf{i}_{\mathrm{ICE,EM}}$, the shift strategy is adapted and the powertrain model is executed, where the resulting fuel consumption V_{fuel} or energy consumption E represents the cost function for the optimization. In order to consider a wide range of vehicle speeds and accelerations, the test cycles WLTP, Urban Dynamometer and FTP 75 are considered and for the cost function the average consumption is used.

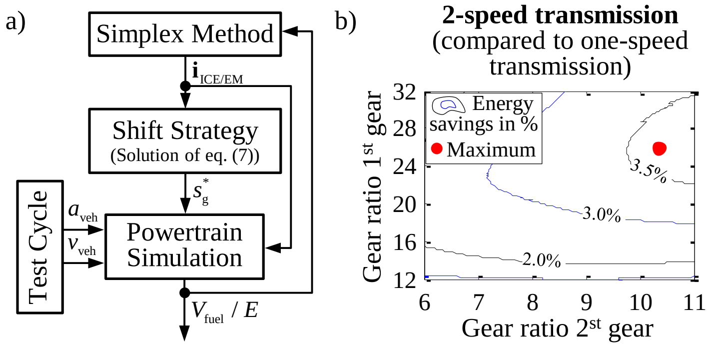

	1 speed $\bar{E}$ $\frac{\mathrm{kwh}}{100\mathrm{km}}$	2 speeds p_2 %	3 speeds p_3 %	4 speeds p_4 %
Energy cons.	17.18	**-3.55**	**-3.91**	**-4.09**
1st gear	10.37	25.90	31.71	34.88
2nd gear	--	10.37	18.65	21.10
3rd gear	--	--	10.37	14.01
4th gear	--	--	--	9.59

Figure 4: a) Optimization of the transmission ratios in terms of a minimal fuel and energy consumption, respectively and b) Optimization results of multi-speed transmissions for the electric motor operation.

Figure 4b shows the energy savings, which can be obtained by multi-speed transmissions for the electric motor operation. The diagram shows the energy savings as function of the transmission ratios for a two-speed transmission and the table contains the optimized energy consumptions as well as the corresponding transmission ratios for a one- to four-speed transmission. In order to ensure that the electric motor can be operated up to a vehicle speed of 180 km/h, the transmission ratio of the highest gear is constrained to values smaller than 10.37. The table shows that the benefit of a two-speed transmission is up to 3.5% energy saving, whereas the benefit of each additional speed becomes drastically smaller.

The fuel savings, which can be obtained by multi-speed transmissions for the ICE operation are shown in Figure 5, where the diagrams depict the functions of fuel saving for a two- and three-speed transmission. In order to enable a maximum vehicle speed of 180 km/h, the transmission ratio of the highest gear is always 3.47. Since not all operating conditions of the vehicle can be driven by the ICE, an imaginary series hybrid mode is introduced, where the ICE is decoupled from the final drive and operated according to the characteristic of minimal fuel consumption. It is assumed that the ICE must produce 30% more mechanical power than required at the final drive. The table in Figure 5 shows that compared to a one-speed transmission, the benefit of a two-speed transmission is up to 8.1% fuel saving and of a three speed transmission up to 9.5%. Each additional speed increases the fuel saving but the benefit compared to a lower number of speeds decreases.

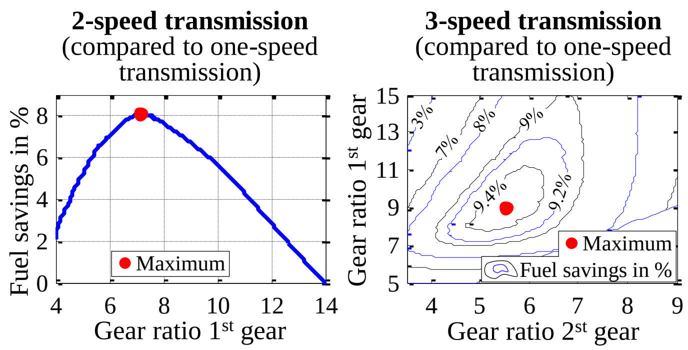

	1 speed $\bar{V}$ $\frac{\mathrm{l}}{100\mathrm{km}}$	2 speeds p_2 %	3 speeds p_3 %	4 speeds p_4 %	5 speeds p_5 %	6 speeds p_6 %
Fuel cons.	6.2	**-8.1**	**-9.5**	**-10.1**	**-10.5**	**-10.6**
1st gear	3.47	7.13	9.02	12.27	16.62	23.54
2nd gear	--	3.47	5.53	7.41	8.89	10.82
3rd gear	--	--	3.47	5.10	6.23	7.54
4th gear	--	--	--	3.47	4.56	6.01
5th gear	--	--	--	--	3.47	4.53
6th gear	--	--	--	--	--	3.47

Figure 5: Optimization results of multi-speed transmissions for the ICE operation.

For the ICE and the electric motor, the most beneficial number of speeds is two. The additional benefit of every additional speed decreases and it must be taken into account that the transmission becomes more complex when the number of speeds rises. Due to a complex transmission, power losses and weight will increase which might vanish the small increment of fuel savings for an additional speed. It must also be considered that due to the separate consideration of the ICE and the electric motor, the transmission ratios are an estimation only. More accurate results can be obtained by considering the combined operation of the ICE and electric motor. The results shown in Figure 4 and Figure 5 are taken as a basis for the development of a new DHT concept and an additional optimization step, where the combined operation is considered.

4 New Transmission Concept

Based on the results of the optimizations in chapter 3, the new transmission concept depicted in Figure 6 was developed [8]. A two-speed transmission for the ICE and the electric motor operation is chosen, since it enables the biggest benefit in terms of fuel and energy savings by means of the lowest complexity of the transmission. Due to the fact that at low speeds the vehicle can only be propelled with the electric motor, it must be ensured that even if the battery is discharged, the operation of the vehicle is still possible. Therefore, the new concept enables a continuous variable transmission (CVT) mode. In this mode, the rotational speeds of the ICE and electric motor are superimposed by means of a planetary gear, which enables to control the rotational speed of the ICE with the speed of the electric motor. The speeds of the ICE can be adjusted continuously as a function of the speeds of the electric motor and the final drive (see, Eq. (10)). The design of the transmission ensures that the electric motor operates as a generator in CVT mode until an appropriate vehicle speed is reached where the ICE mode can be activated.

According to Figure 6, the first planetary gear is used to change the operation mode and the second planetary gear (epicyclic gear with two sun gears) is used to change the gear (two-speed transmission). If the dog clutch K_2 is disengaged, the rotational speeds of the ICE and electric motor are superimposed and the powertrain operates in CVT-Mode. Otherwise, if K_2 is engaged, the planets are blocked and the whole planetary gear rotates as one common body. In this case, the electric driving mode, the ICE mode or the parallel hybrid mode can be active. When the ICE is used for propulsion, the clutch K_1 must be engaged. The brake B activates the first gear and the multi-plate clutch K_3 the second gear. Each operation mode can be driven in two different speeds.

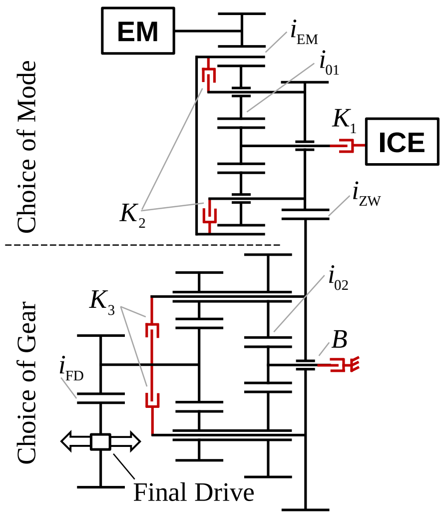

Modes: × Clutch or brake engaged

	CVT1 (s_m=1)	CVT2 (s_m=2)	ICE1/ PAR (s_m=3)	ICE2/ PAR (s_m=4)	EM1 (s_m=5)	EM2 (s_m=6)
Clutch K_1	×	×	×	×		
Dog Clutch K_2			×	×	×	×
Clutch K_3		×		×		×
Brake B	×		×		×	

Figure 6: New transmission concept and the information of how to activate the available operation modes.

The overall transmission ratio of the ICE mode is

$$i_{\mathrm{ICE,FD}} = \frac{T_{\mathrm{FD,ICE}}}{T_{\mathrm{ICE}}} = \frac{-\omega_{\mathrm{ICE}}}{\omega_{\mathrm{FD}}} = \tilde{i} \cdot i_{\mathrm{PG2}} \tag{8}$$

and of the electric motor mode is

$$i_{\mathrm{EM,FD}} = \frac{-T_{\mathrm{FD,EM}}}{T_{EM}} = \frac{\omega_{\mathrm{EM}}}{\omega_{\mathrm{FD}}} = i_{\mathrm{EM}} \cdot \tilde{i} \cdot i_{\mathrm{PG2}} \tag{9}$$

with $\tilde{i} = i_{\mathrm{FD}} \cdot i_{\mathrm{ZW}}$ and $i_{\mathrm{PG2}} = 1/\left(1-i_{02}\right)$ for the first gear and $i_{\mathrm{PG2}} = 1$ for the second gear. The final drive torque T_{FD} will be composed of the sum of $T_{\mathrm{FD,ICE}}$ and $T_{\mathrm{FD,EM}}$.

Considering the CVT mode, the overall transmission ratio regarding the rotational speed of the ICE ω_{ICE} is a function of the rotational speed of the electric motor ω_{EM} and the final drive ω_{FD}

$$i_{\omega,\mathrm{CVT,FD}} = \frac{\omega_{\mathrm{ICE}}}{\omega_{\mathrm{FD}}} = \frac{-1}{i_{01} \cdot i_{\mathrm{EM}}} \frac{\omega_{\mathrm{EM}}}{\omega_{\mathrm{FD}}} - \frac{1+i_{01}}{i_{01}} \cdot \tilde{i} \cdot i_{\mathrm{PG2}} \tag{10}$$

which enables to adjust the rotational speed of ICE ω_{ICE} for a given final drive speed ω_{FD} by means of ω_{EM}. According to the transmission ratio regarding the torques

$$i_{\mathrm{T,CVT,FD}} = \frac{-T_{\mathrm{FD}}}{T_{\mathrm{ICE}}} = \frac{i_{01} \cdot T_{\mathrm{FD}}}{T_{\mathrm{EM}}} = -\tilde{i} \cdot i_{\mathrm{PG2}} \cdot \left(1+i_{01}\right), \tag{11}$$

the torques of the ICE T_{ICE} and the electric motor T_{EM} must fulfil the torque equilibrium of the planetary gear.

5 Optimization: Transmission Ratios

In order to determine the optimal transmission ratios of the new transmission concept, a further optimization step is carried out. The transmission model used for the optimization considers the concept in Figure 6, where the torques and angular speeds are calculated according to the transmission ratios of the planetary and spur gears. As an initial parameterization, the transmission ratios obtained in chapter 3 are used. For the optimization, the minimal fuel consumption for a given set of transmission ratios and test cycles has to be calculated. This can only be enabled, if the combined operation of the ICE and the electric motor is considered (ICE/Parallel or CVT-Mode) and controlled optimally. Generally, an optimal control trajectory for the powertrain $\mathbf{u}^*(t)$ must be determined, which solves the optimization problem

$$\begin{aligned}
&\min_{\mathbf{u}(t)} \left\{ J = \int_0^{t_e} \dot{m}_{\mathrm{f}} \left(T_{\mathrm{ICE}}, \omega_{\mathrm{ICE}}\right) dt \right\} \\
&\dot{q} = f_{\mathrm{Batt}} \left(P_{\mathrm{el}} \left(T_{\mathrm{EM}}, \omega_{\mathrm{EM}}\right)\right) \\
&\left[T_{\mathrm{ICE}} \; T_{EM} \; \omega_{\mathrm{ICE}} \; \omega_{EM}\right]^T = \mathbf{f}_{\mathrm{Trans}} \left(T_{\mathrm{FD}}, \omega_{\mathrm{FD}}, \mathbf{u}\right) \\
&q \in \mathcal{X} \;, \; \mathbf{u} = [s_{\mathrm{m}} \; \tilde{u}]^T \in \mathcal{U}^2
\end{aligned} \tag{12}$$

with the cost function J and the duration of the test cycle t_{e}. The control vector $\mathbf{u}$ summarizes the operation mode s_{m} and the variable control input for the electric motor

$$\tilde{u} := \begin{cases} \tilde{\omega}_{\mathrm{EM}} & , s_{\mathrm{m}} = 1 \vee 2 \\ \tilde{T}_{\mathrm{EM}} & , s_{\mathrm{m}} = 3 \vee 4 \\ 0 & , s_{\mathrm{m}} = 5 \vee 6 \end{cases} \tag{13}$$

where the allocation of the shown numbers can be found in Figure 6. The optimal control trajectory $\mathbf{u}^*(t)$ will satisfy the state equation $\dot{q}$ as well as the state space constraints $\mathcal{X}$ and control space constraints $\mathcal{U}^2$. In this contribution, a combination of the optimization methods Dynamic Programming (DP) and Calculus of Variations (CoV) is applied, where DP determines the discrete input s_{m} and CoV the continuous input $\tilde{u}$. This method was already presented in [9] and enables time-efficient optimizations. However, since the method was applied on a parallel hybrid vehicle with a six-speed transmission for the ICE, it had to be adapted to the new more complex vehicle configuration. In the next sections, the basics of CoV and DP as well as the combination of both are described. Finally, the results obtained by applying the proposed method for the optimization of the transmission ratios are presented.

5.1 Calculus of Variations (CoV)

The basics of the CoV are presented in [10]. The optimal continuous input $\tilde{u}^*$ is obtained by minimizing the Hamiltonian function

$$\mathcal{H} = \dot{m}_{\mathrm{f}}\left(T_{\mathrm{FD}}, \omega_{\mathrm{FD}}, s_{\mathrm{m}}, \tilde{u}\right) + \lambda \cdot \dot{q}\left(T_{\mathrm{FD}}, \omega_{\mathrm{FD}}, s_{\mathrm{m}}, \tilde{u}\right) \tag{14}$$

in terms of the input $\tilde{u}$. It is assumed that the Lagrange multiplier λ is known in advance and the optimal solution $\tilde{u}^*$ does not have to be bounded to the limits of the control space constraint $\mathcal{U}$. Furthermore, the final drive torque T_{FD} and angular velocity ω_{FD} as well as the operation mode s_{m} are considered here as constants. Then a potential minima of (14) is obtained by fulfilling the necessary conditions

$$\frac{\partial \mathcal{H}}{\partial \tilde{u}} = 0 \;\Leftrightarrow\; \tilde{u} = f_{\tilde{u}}(\lambda) \tag{15}$$

$$-\frac{\partial \mathcal{H}}{\partial q} = \dot{\lambda} \tag{16}$$

where (15) is rearranged according to $\tilde{u}$. In this case, since the Lagrange multiplier λ is assumed to be known, the second condition (16) is not required and the optimal solution $\tilde{u}^*$ can be calculated directly by means of (15). However, it must be taken into account, that (15) is only the optimal solution $\tilde{u}^*$, if it also fulfills the sufficient condition for an extrema. According to [11], the sufficient condition is always fulfilled when the cost function J is convex regarding $\tilde{u}$. In order to obtain a convex cost function, the original data map of the fuel flow rate of the ICE (see Figure 3) is approximated by the parabolic function

$$\dot{m}_{\mathrm{f,convex}}\left(T_{\mathrm{ICE}}, \omega_{\mathrm{ICE}}\right) = a_2\left(\omega_{\mathrm{ICE}}\right) \cdot T_{ICE}^2 + a_1\left(\omega_{\mathrm{ICE}}\right) \cdot T_{\mathrm{ICE}} + a_0\left(\omega_{\mathrm{ICE}}\right) \tag{17}$$

where the coefficients are a function of the rotational speed. It is required that (17) is a convex function of T_{ICE} because it is directly affected by the input $\tilde{u}$. In order to have an analytic equation for the Hamiltonian function (14), the power losses of the electric motor are also approximated by a convex function

$$P_{\mathrm{EM,loss,convex}}\left(T_{\mathrm{EM}}, n_{\mathrm{EM}}\right) = b_2\left(\omega_{\mathrm{EM}}\right) \cdot T_{\mathrm{EM}}^2 + b_1\left(\omega_{\mathrm{EM}}\right) \cdot T_{\mathrm{EM}} + b_0\left(\omega_{\mathrm{EM}}\right). \tag{18}$$

A further approximation is made, by using the convex state equation

$$\dot{q}_{\mathrm{convex}} = i_{\mathrm{Batt}}\left(P_{\mathrm{el}}\right) = c_2 \cdot P_{\mathrm{el}}^2 + c_1 \cdot P_{\mathrm{el}} + c_0 \tag{19}$$

where the influence of the SoC on the battery current i_{Batt} is neglected. Considering (17)-(19), the Hamiltonian function (14) becomes independent of q and the derivation of λ in (16) becomes zero. This means that the Lagrange multiplier λ must be a constant value.

5.2 Dynamic Programming (DP)

The general application of the DP method is presented in [12]. For the intended application, the Hamiltonian function is considered as cost function

$$\min_{u_{\mathrm{m}}(t)} \left\{ J_{\mathrm{DP}} = \int_0^{t_{\mathrm{e}}} \mathcal{H}\left(T_{\mathrm{FD}}, \omega_{\mathrm{FD}}, \lambda, s_{\mathrm{m}}\right) dt \right\} \tag{20}$$

and the operation mode as a state variable

$$s_{\mathrm{m,k+1}} = s_{\mathrm{m,k}} + u_{\mathrm{m,k}} \tag{21}$$

with the discrete control input $u_{\mathrm{m,k}} \in \mathbb{N} \subseteq \{-5, ..., 5\}$. It is still assumed that the constant Lagrange multiplier λ is known in advance. Then the Hamiltonian function can be evaluated for a given operation mode s_{m} by means of the CoV (Eq. (14) and (15)) and the DP algorithm can determine a trajectory for the operation mode s_{m} which yields a minimal Hamiltonian function. The optimization problem is considered time-discrete, where for each time step $t_{\mathrm{k}} = k \cdot T$ the local optimization problem

$$\mathbf{J}_{\mathrm{DP,k}}\left(\mathbf{s}_{\mathrm{m,k}}\right) = \min_{\mathbf{u}_{\mathrm{m}}} \left\{ \mathbf{J}_{\mathrm{DP,k+1}}\left(\mathbf{s}_{\mathrm{m,k+1}}\right) + \mathbf{H}\left(T_{\mathrm{FD,k}}, \omega_{\mathrm{FD,k}}, \lambda, \mathbf{s}_{\mathrm{m,k}}\right) \cdot T \right\} \tag{22}$$

is solved for the matrix $\mathbf{H}$ containing the Hamiltonian function values for all possible states $\mathbf{s}_{\mathrm{m}}$ and inputs $\mathbf{u}_{\mathrm{m}}$. Equation (22) is solved backwards in time from $k = N-1$ to $k = 0$ with the initial costs $\mathbf{J}_{\mathrm{DP,N}} = 0$. The result is an optimal control vector $\mathbf{u}^*_{\mathrm{m,k}}$ and the minimal accumulated costs for each state within the state grid vector $\mathbf{s}_{\mathrm{m,k}}$. The optimal inputs $\mathbf{u}^*_{\mathrm{m,k}}$ are also allocated to the state grid vector and are saves in a new matrix

$$\mathbf{U}^*_{\mathrm{m,k}}\left(\mathbf{s}^*_{\mathrm{m,k}}\right)=\mathbf{u}^*_{\mathrm{m,k}}\,. \tag{23}$$

After completing the backward calculation, the optimal control input trajectory u^*_{m} is determined by extracting the optimal inputs u^*_{m} from the matrix (23) according to operation mode $s_{\mathrm{m,k}}$

$$u^*_{\mathrm{m,k}}=\mathbf{U}_{\mathrm{m,k}}\left(s_{\mathrm{m,k}}\right). \tag{24}$$

Equation (24) is processed forward in time from $k=0$ to $k=N-1$, where the next operation mode $s_{\mathrm{m,k+1}}$ is calculated according to (21) by means of the result of (24).

5.3 DP and CoV Combined

Figure 7a shows the algorithm for the optimization of the vehicle operation by means of the combination of DP and CoV. The constant Lagrange multiplier λ is still unknown and must be determined. According to Figure 7c, it affects the initial State of Charge SoC_0 and only the correct λ will satisfy the desired initial condition SoC^*_0. The solution is determined by means of Regula Falsi method, where the whole algorithm comprising DP and CoV must be executed in order to evaluate SoC_0.

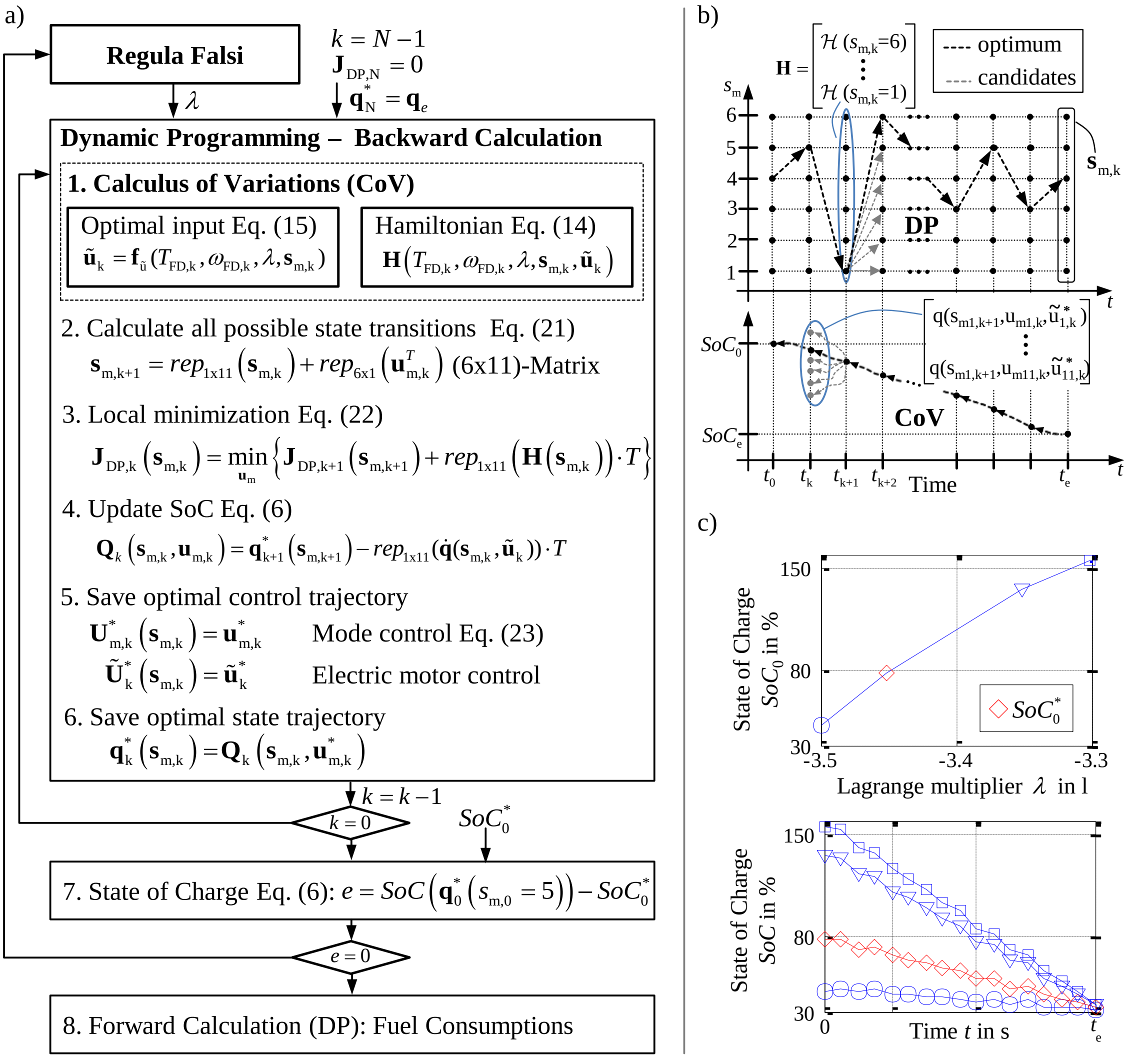

Figure 7: a) Algorithm for the optimization of the vehicle operation, b) schematic representation of algorithm and c) characteristics of the Lagrange multiplier λ and the resulting initial values for the SoC.

The algorithm which combines DP and CoV consists basically of the backward calculation of the DP. It begins at $k = N - 1$ and the first step is to apply the CoV in order to determine the Hamiltonian functions $\mathbf{H}$ for all operation modes of the state grid $\mathbf{s}_{\mathrm{m,k}}$ and the current final drive torque $T_{\mathrm{FD,k}}$ and speed $\omega_{\mathrm{FD,k}}$. In the second step all possible state transitions from $\mathbf{s}_{\mathrm{m,k}}$ to $\mathbf{s}_{\mathrm{m,k+1}}$ are calculated. Figure 7b illustrates the state transitions from $t_{\mathrm{k+1}}$ to $t_{\mathrm{k+2}}$ for the initial state $s_{\mathrm{m,k}} = 6$ (grey arrows in upper part). Each transition corresponds to one input in $\mathbf{u}_{\mathrm{m,k}}$, where the input, which causes less costs is chosen to be optimal (black arrow in upper part of Figure 7b). The choice of the optimal input is made in the third step, by minimizing the accumulated costs $\mathbf{J}_{\mathrm{DP,k}}$. The result is the optimal control vector $\mathbf{u}^{*}_{\mathrm{m,k}}$, which contains the optimal input for each operation mode of the state grid $\mathbf{s}_{\mathrm{m,k}}$. The optimal input control for the operation states $\mathbf{u}^{*}_{\mathrm{m,k}}$ and the electric motor $\tilde{\mathbf{u}}^{*}_{\mathrm{k}}$ are saved in the fifth step. In order to evaluate the current SoC_{k}, the electric charge for all combinations of the states $\mathbf{s}_{\mathrm{m,k}}$ and inputs $\mathbf{u}_{\mathrm{m,k}}$ is determined and saved in $\mathbf{Q}_{\mathrm{k}}$ (step four). At the bottom of Figure 7b an exemplary characteristic of the SoC is shown. Generally, more than one characteristic will exist and for each characteristic and time step the optimal transition must be determined. This is solved by extracting the solutions which belong to the optimal control vector $\mathbf{u}^{*}_{\mathrm{m,k}}$ (see, step six in Figure 7a).

After completing the backward calculation, SoC_0 is determined in step seven (electric driving is the initial operation state $s_{\mathrm{m,0}} = 5$). If the deviation regarding the desired value SoC^{*}_{0} becomes small enough, the resulting fuel consumption is calculated in step eight by means of the forward calculation and the matrices saved in step five.

5.4 Optimization Results

The algorithm shown in Figure 7 enables the determination of the fuel consumption for a given set of test cycles. For the optimization of the transmission ratios of the new transmission concept the test cycles FTP 75, Urban Dynamometer and WLTP are considered. All test cycles are repeated until the overall distance is equal to approximately 200km (ensures that the battery is discharged). The operation of the powertrain is optimized for the considered test cycles and a predefined range of the transmission ratios of the first ICE-mode and the second electric driving mode. Due to the properties of the new transmission concept, all other transmissions ratios are defined by means of those two. Figure 8 shows the fuel savings as a function of the transmission ratios. It is compared to the fuel saving of the new transmission concept, which was parametrized according to the results obtained in chapter 3. It turned out, that due to the additional optimization of the transmission ratios, a fuel saving of up to 1.4% is obtained compared to the parametrization according to the separated consideration of ICE and electric motor.

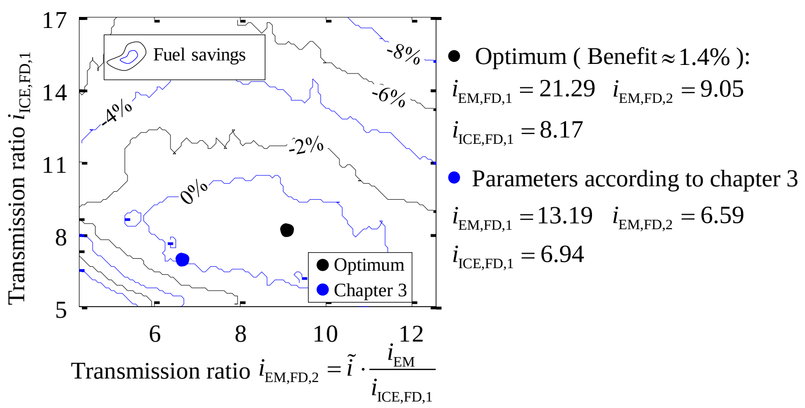

Figure 8: Optimization results regarding the transmission ratios of the new transmission concept.

6 Concept Evaluation

A model-based evaluation of the new transmission concept with the optimized transmission ratios is carried out in this chapter. As reference, the powertrain concept shown in Figure 9a is chosen. It corresponds to the concept of the Mitsubishi Outlander PHEV. Both powertrains have the same ICE and electric motor for traction (the reference requires a second motor for the series hybrid mode). The vehicle parameterizations of both powertrain models are chosen equally and similar to the Mitsubishi Outlander. In order to obtain accurate simulation results, estimated weights of the overall powertrains and the power losses within the transmissions are considered. The efficiency of each gear pair within the transmissions is chosen to be 0.99 and the drag losses of the clutches and brakes are assumed to be 0.5Nm (stationary only). The new transmission concept is heavier than the reference concept but requires only one electric motor. Therefore, the overall mass of the vehicle with the new powertrain concept weighs less than the reference ($\approx$30kg).

For the comparison of both concepts, transmission models which consider power losses are used and the Dynamic Programming is applied to determine the optimal control of the powertrain and thus the minimal fuel consumption is obtained for both concepts. The method is carried out with a high resolution and is applied to the test cycles: FTP 75, Urban Dynamometer and WLTP. All test cycles are repeated until an overall distance equal to approximately 200km is driven. Figure 9c shows the simulated fuel consumptions of the two powertrain models. Depending on the test cycle, the new transmission concept enables fuel savings between 4.4% and 9.7%. Despite the more complex transmission architecture (higher power losses and weight), fuel savings can be achieved for each driving cycle. The first reason is the increased degree of freedom in terms of the transmission control, which enables the ICE and the electric motor to be operated more efficiently. The second reason is the decreased weight of the vehicle due to the usage of only one electric motor.

a) b)

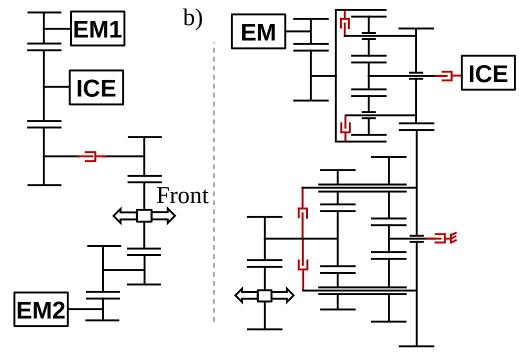

c)

Test Cycle	reference a)	new concept b)	relative difference in %
	fuel consumption in l/100km		
FTP 75	3.412	3.146	**-7.79**
Urban Dyna-mometer	3.213	2.900	**-9.74**
WLTP	3.809	3.641	**-4.41**

Figure 9: a) Reference powertrain concept, b) new powertrain concept and c) simulation results.

The calculated fuel savings are the theoretical minimum. Considering the real vehicle application, the fuel consumptions will increase because the simulation does not consider the powertrain dynamics and the optimal control used here is not applicable since the operation modes can oscillate to fast for operating the real transmission. Nevertheless, these investigations provide important information for the development of the new transmission and powertrain concept for PHEVs, respectively.

7 Conclusion

In this contribution the model-based development and optimization of a new transmission concept for PHEVs is presented. A stationary powertrain model with a vehicle parameterization similar to the Mitsubishi Outlander is used to investigate the benefits of multi-speed transmissions for the ICE and the electric motor. First, the propulsion of the vehicle with the ICE and electric motor is considered separately, in order to estimate the optimal number of speeds. It turned out that two-speed transmissions are most beneficial. Based on these results, a new transmission concept for PHEVs is presented, which enables an electric driving mode, an ICE and parallel hybrid mode and a CVT mode. Each mode can be operated in two speeds. For the new concept, a further optimization step is carried out, where the transmission ratios are optimized. A model-based concept evaluation showed that the new and optimized transmission concept enables a theoretical improvement of 7.3% fuel saving (in average) compared to a transmission concept with fixed gear ratios for the ICE and electric motor operation.

Acknowledgments

This contribution is accomplished within the project PHEVplus (FKZ: 01MY13004B), funded by the Federal Ministry of Economics and Energy (BMWi) and in cooperation with GKN Driveline International GmbH, www.phevplus.de.

References

[1] D. Karbowski, S. Pagerit, J. Kwon, A. Rousseau, et al., *"Fair" Comparison of Powertrain Configurations for Plug-In Hybrid Operation Using Global Optimization*, SAE Technical Paper, 2009-01-1334, 2009.

[2] G. Goppelt, *Das DHT Hybridgetriebe neu definiert*, ATZ – Automobiltechnische Zeitschrift, 7-8, 2016.

[3] M. Taniguchi, T. Yashiro, K. Takizawa, S. Baba, et al., *Development of New Hybrid Hybrid Transaxle for Compact-Class Vehicles*, SAE Technical Paper, 2016-01-1163, 2016.

[4] B.M. Conlon, T. Blohm, M. Harpster, A. Holmes, et al., *The next Generation "Voltec" Extended Range EV Propulsion System*, SAE International Journal of Alternative Powertrains, 4(2), pages 248-259, 2015.

[5] T. Gassmann, M. Aikawa, *GKN Multi-Mode eTransmission for Premium Hybrid Vehicles*, 12th International CTI Symposium, 2013.

[6] T. Markel, et al., *ADVISOR: A Systems Analysis Tool for Advanced Vehicle Modeling*, Elsevier – Journal of Power Sources, Vol. 110, pages 255-266, 2002.

[7] S. Geng, S. Herber, W. Hildebrandt, T. Schulte, *Powertrain Simulation and Optimization of a Multimode Transmission*, FISITA World Automotive Congress, F2016-THBE-005, 2016.

[8] S. Herber, *PHEVplus: Effizienzsteigerndes DHT für Plug-In Hybridanwendungen*, 17. Internationaler VDI-Kongress - Getriebe in Fahrzeugen, 2017.

[9] V. Ngo, T. Hofman, M. Steinbruch, A. Serrarens, *Optimal Control of the Gearshift Command for Hybrid Electric Vehicles*, IEEE Transactions on Vehicular Technology, vol. 61, No. 8, 2012.

[10] D. S. *Naidu, Optimal Control Systems*, Electrical Engineering Textbook Series, 2003.

[11] N. Kim, A. Rousseau, *Sufficient conditions of optimal control based on Pontryagin's minimum principle for use in hybrid electric vehicles*, Journal of Automobile Engineering, 2012.

[12] D. P. Bertsekas, Dynamic Programming and Optimal Control Volume I, Athena Scientific, 2005.